Valence Determination by Electron Energy Loss Spectroscopy of the Multi-Valence Metal Chromium

T. L. Daulton* and B. J. Little**

*Marine Geosciences Division, **Oceanography Division
Naval Research Laboratory, Stennis Space Center, MS 39529, USA

Chromium is a redox active $3d$ transition metal with a wide range of valences (-2 to +6) that control the geochemistry and toxicity of the element. A variety of Cr-bearing minerals [1] are found in meteorites of all petrographic classes [2], lunar basalts [3], Martian rocks, and the Earth, recording valuable information concerning geochemical conditions of mineralization. Natural weathering of Cr-bearing minerals [4] and fallout of volcanic ash release Cr into the terrestrial environment. Furthermore, Cr compounds are widely used in numerous industrial processes [5] which can discharge toxic Cr complexes in soils/sediments and surface/ground waters, as well as the atmosphere in the form of aerosols. Therefore, techniques that measure Cr valence are important bio/geochemical tools. Until now, all established methods to determine Cr valence were bulk techniques with many specific to a single, or at best, only a few oxidation state(s). We report electron energy loss spectroscopy (EELS) techniques that, unlike other methods, can determine Cr valence at high-spatial resolution (nm-scale) over a wide valence range, Cr(0) to Cr(VI).

In this work, the fine structure of Cr-$L_{2,3}$ edges was parametrized by measurement of the chemical shift of the L_3 edge and the ratio of integrated intensity under the L_3 and L_2 edges (Table 1). These parameterizations were correlated to Cr valence for a large suite of standards (Fig. 1). Valence of an unknown can be determined by comparing its fine structure parameterizations to that of the standards. Measurement of the L_3/L_2 ratio is highly dependent on the post-edge background subtraction. The background was modeled by a fit to a 2 eV wide window positioned 4.8 eV above the L_2 maximum. The fit was extrapolated to the L_2 maximum where a step was inserted and then was extrapolated to the L_3 maximum. A second step function was inserted at the L_3 maximum and set to zero below the maximum (Fig. 2). The ratio for the step heights was initially set as 2, but was refined by iteration by assigning the step height the value of the L_3/L_2 ratio determined after each iteration. Intensity of the L edges was measured by integrating a 5 eV wide region centered with respect to the edge maxima.

Our results demonstrate that other factors in addition to valence, e.g. crystal field splitting (i.e, atom coordination, low- or high-spin configuration), spin-orbit interactions, atomic coulomb repulsion, and exchange effects, can significantly influence the fine structure of Cr-$L_{2,3}$ adsorption edges. Consequently, measurement of the L_3 peak position and the ratio of L_3/L_2 integrated peak intensity must be used together to unambiguously determine Cr valence if the full range of oxidation states is considered. However, even with two parameterizations it is difficult to distinguish Cr(IV) and low-spin Cr(II) compounds from Cr(III). Nevertheless, when Cr is known divalent, low- and high-spin d^n orbital configurations can be readily distinguished.

References:
[1] V. M. Burns & R. G. Burns, *Geochim. Cosmochim. Acta* **39**, 903-910 (1975).
[2] T. E. Bunch & E. Olsen, *Geochim. Cosmochim. Acta* **39**, 911-927 (1975).
[3] S. R. Sutton *et al., Geochim. Cosmochim. Acta* **57**, 461-468 (1993).
[4] J. Robles-Camacho & M. Armienta, *J. Geochem. Explor.* **68**, 167-181 (2000).
[5] M. E. Losi *et al., Rev. of Environ. Contam. & Toxicol.* **136**, 91-121 (1994).

Table 1.
Fine Structure Parameterizations

Standard	L_3 Peak (eV)	L_3/L_2
Cr(0)		
$Cr_{23}C_6$	578.03 (5)	1.498 (3)
$Cr(CO)_6$	579.06 (7)	1.520 (7)
Cr	577.18 (2)	1.525 (3)
Cr(I)		
$(C_6H_6)_2CrI$	576.87 (3)	1.798 (6)
Cr(II)		
$[(CH_3)_4C_5H]_2Cr$	578.43 (4)	1.715 (4)
$Cr_2(CH_3COO)_4 \cdot 2(H_2O)$	578.55 (3)	1.720 (2)
$[(CH_3)_5C_5]_2Cr$	578.35 (2)	1.757 (3)
CrSe	576.65 (5)	2.004 (13)
$CrCl_2$	577.11 (4)	2.184 (17)
CrF_2	576.78 (3)	2.246 (14)
Cr(III)		
$CrPO_4 \cdot 4H_2O$	579.74 (6)	1.546 (3)
$KCr(SO_4)_2 \cdot 12H_2O$	579.77 (4)	1.559 (5)
$CrCl_3$	578.13 (2)	1.638 (3)
$(Fe,Mg)(Cr,Al,Fe)_2O_4$	578.89 (2)	1.646 (2)
$NdCrO_3$	579.35 (3)	1.675 (7)
$LaCrO_3$	578.71 (2)	1.704 (4)
$Cr_3(CH_3COO)_7(OH)_2$	578.47 (2)	1.709 (2)
Cr_2O_3	578.81 (3)	1.712 (5)
Cr(IV)		
CrO_2	579.70 (3)	1.548 (2)
Cr(V)		
$NdCrO_4$	580.43 (3)	1.414 (4)
Cr(VI)		
$PbCrO_4$	581.85 (7)	1.370 (5)
$K_2Cr_2O_7$	582.83 (3)	1.408 (6)
K_2CrO_4	581.77 (2)	1.474 (4)
Na_2CrO_4	582.26 (3)	1.475 (6)

Spectrometer calibrated to yield 855.0 eV for Ni-L_3 edge maximum of NiO. Standard error of mean (for upwards of 30 measurements) is given by (n), e.g. for $Cr_{23}C_6$: 1.498 (3) = 1.498 ± 0.003.

Cr Valence Correlation Plot

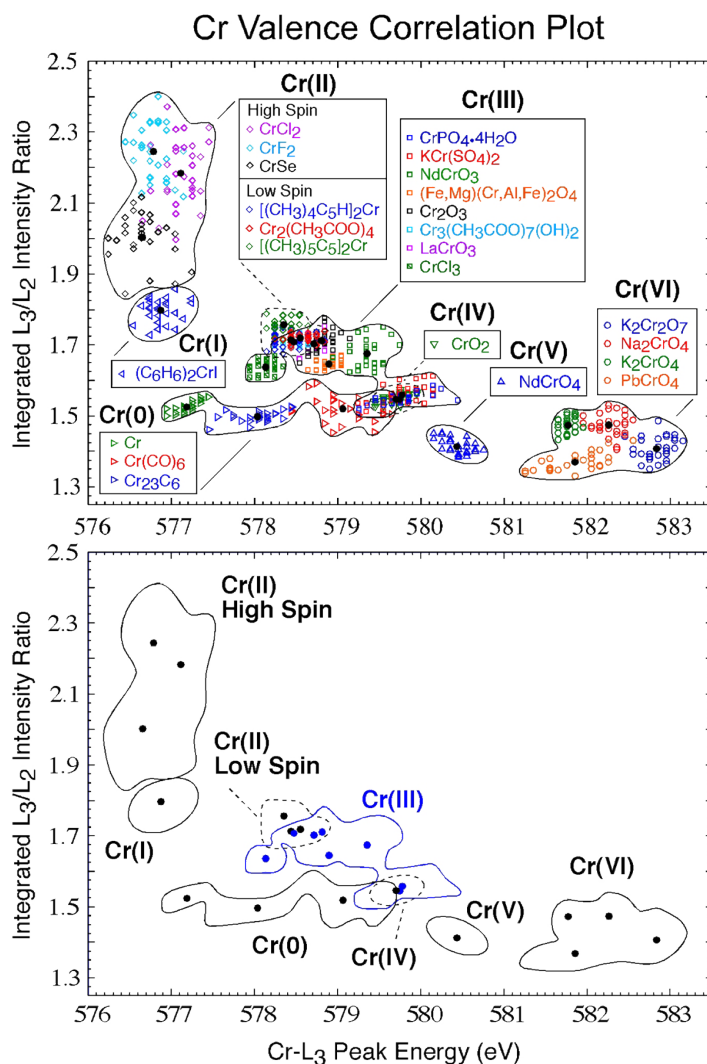**Figure 1.** The correlation between measured L_3/L_2 integrated-peak intensity ratios and L_3 peak positions for Cr oxidation-state standards. The black, solid circles represent the mean of the data for a particular Cr standard. The regions bounded by closed curves are visual guides.

Post-Edge Background

Figure 2. Post-edge background subtraction method used to measure the L_3/L_2 ratio. The bold line is the modeled background determined by a fit to a 2 eV wide window that starts 4.8 eV above the L_2 maxima.